

Nuclear transition induced by low-energy unscreened electron inelastic scatteringG. Gosselin, N. Pillet, V. Méot, and P. Morel
CEA, DAM, DIF F-91297 Arpajon, France

A. Ya. Dzyublik

Institute for Nuclear Research, National Academy of Sciences of Ukraine, Kiev, Ukraine

(Received 18 September 2008; published 14 January 2009)

In this work, we have evaluated the unscreened electron inelastic scattering cross sections in the 1–100 keV range with a second order perturbation theory. The WKB approximation and DWBA calculations for low-energy electrons encountered show less than a 3% difference. Applications have been performed for two nuclei, namely ^{110}Ag and ^{201}Hg .

DOI: [10.1103/PhysRevC.79.014604](https://doi.org/10.1103/PhysRevC.79.014604)

PACS number(s): 23.20.Nx, 25.30.Dh

I. INTRODUCTION

In a hot dense plasma, the lifetime of a nuclear level may significantly be altered [1,2] in comparison with the lifetime of an isolated nucleus. The large number of photons and free electrons modifies the environment in which an excited level of the nucleus naturally decays under laboratory conditions through spontaneous emission and internal conversion (IC), thus modifying its lifetime. New decay modes appear such as induced photon emission, free electron inelastic scattering, and bound internal conversion. The lifetime depends on excitation processes which can repopulate the excited level, leading to a modification of its lifetime [3]. These considerations may be of great interest, either in a laser heated plasma [4–7], or in astrophysical plasmas [8–11].

The main couples of electromagnetic excitation and decay processes [12] are photon absorption and photon emission (both spontaneous and induced), nuclear excitation by electron capture (NEEC) [13], where a free electron is captured on an empty state of an atomic shell, and internal conversion, nuclear excitation by electronic transition (NEET) [14], and bound internal conversion (BIC), and inelastic and superelastic electron scattering. For this latter process, all free electrons in a plasma whose energy is higher than the nuclear transition energy are available to excite the nucleus. Even though the expected cross sections are small, usually well under 10^{-30} cm², the high number of free electrons in a plasma will ensure that the corresponding transition rate is significant. Electron inelastic scattering has been extensively studied [15–19] for energy in the MeV range and above, but no model has been specifically developed to address lower energy electrons with energy in the keV range. The main problem lies in the calculation of the radial matrix element, whose determination is much more complex at low energy, which leads to serious numerical difficulties. In this paper, we extend a well-known model [20] to describe inelastic electron scattering at low energy. As a first step, we only consider an unscreened potential, which allows analytic calculations. However, we provide some clues of the effect of screening, which may play a major role in describing the cross section near threshold.

The paper is organized as follows. In Sec. II, we recall the basics of the quantum perturbation theory applied to electron

inelastic scattering. It provides an expression of the cross section which only depends on the choice of the electron wave functions. We consider the use of distorted wave functions in the framework of the distorted wave born approximation (DWBA) method. We solve the radial wave equation by two different methods: the approximate Wentzel-Kramers-Brillouin (WKB) solution and the exact solution which uses Coulomb wave functions. In Sec. III, we evaluate inelastic scattering cross sections of the first excited level ($t_{1/2} = 660$ ns) of ^{110}Ag and the isomer ($t_{1/2} = 81$ ns) of ^{201}Hg located at 1.565 keV in the 1–100 keV energy range. Summary and conclusions are given in Sec. IV, where we elaborate on the best way to use these cross sections under plasma conditions.

II. COULOMB EXCITATION CROSS SECTION

We consider the quantum-mechanical treatment of electromagnetic excitation of nuclei induced by electron inelastic scattering, assuming an unscreened electrostatic potential of the nucleus.

As in Ref. [20], the first order perturbation method is used to derive the Coulomb excitation cross section. The system is composed of an incident electron, a nucleus and a quantized electromagnetic field represented in the Coulomb gauge. In this gauge, there are both transversally polarized photons and static Coulomb fields. Only the Coulomb interaction of the incident electron with the nucleus provides the main mechanism of its excitation, while an exchange by photons between the electron and the nucleus gives only small corrections [20]. The nonperturbed Hamiltonian consists of the Hamiltonians of the interacting system of the free electron, nucleus, and radiation field. A fourth term associated with the static point charge interaction between the electron and the nucleus is added. The perturbation Hamiltonian contains three terms corresponding to the interaction between: (i) the radiation field and the nucleus, (ii) the radiation field and the electron, and (iii) a residual Coulomb interaction coming from the charge distribution inside the nucleus. The eigenstates of the nonperturbed Hamiltonian are written as the product of the wave functions of the electron in the Coulomb field, the nucleus and the radiation field. A nonrelativistic treatment is applied

since we are interested in electrons with energies smaller than a few hundred keV. The nuclear recoil is not taken into account.

The total cross section σ is expressed as the sum of electric ($\sigma_{E\lambda}$) and magnetic ($\sigma_{M\lambda}$) components:

$$\sigma = \sum_{\lambda=1}^{\infty} \sigma_{E\lambda} + \sigma_{M\lambda}, \quad (1)$$

where λ denotes the multipolarity of the transition. The expressions for $\sigma_{E\lambda}$ and $\sigma_{M\lambda}$ are [20]:

$$\sigma_{E\lambda} = \left(\frac{Ze}{\hbar v_i} \right)^2 a^{-2\lambda+2} B(E\lambda) f_{E\lambda}(\eta_i, \xi), \quad (2)$$

$$\sigma_{M\lambda} = \frac{v_f}{v_i} \left(\frac{Ze}{\hbar c} \right)^2 a^{-2\lambda+2} B(M\lambda) f_{M\lambda}(\eta_i, \xi), \quad (3)$$

where the indices i and f refer to the initial and final electron states, respectively.

In Eqs. (2) and (3), η is the dimensionless Sommerfeld parameter which characterizes the motion of the electron in the Coulomb field of the nucleus and measures the effective force of the interaction:

$$\eta_i = -\frac{Ze^2}{\hbar v_i}, \quad (4)$$

where Z is the charge of the nucleus and v is the velocity of the incident electron. The parameter ξ is defined as the difference:

$$\xi = \eta_f - \eta_i. \quad (5)$$

The quantity a is half the distance of the closest approach in a head-on collision, namely,

$$a = \frac{Ze^2}{m v_i v_f}. \quad (6)$$

The electric or magnetic cross sections are proportional to the product of the reduced transition probability denoted $B(\lambda)$ [for the evaluation of cross sections, the $B(\lambda)$ values are taken from experimental data] and an electron electric or magnetic excitation function denoted $f_{\lambda}(\eta, \xi)$:

$$f_{E\lambda}(\eta_i, \xi) = \frac{64\pi^2}{(2\lambda+1)^2} k_i k_f a^{2\lambda-2} \sum_{\ell_i \ell_f} (2\ell_i+1)(2\ell_f+1) \times \begin{pmatrix} \ell_i & \ell_f & \lambda \\ 0 & 0 & 0 \end{pmatrix}^2 |M_{\ell_i \ell_f}^{-\lambda-1}|^2, \quad (7)$$

$$f_{M\lambda}(\eta_i, \xi) = \frac{64\pi^2(\lambda+1)}{\lambda(2\lambda+1)} a^{2\lambda-2} \sum_{\ell_i \ell_f} (2\ell_i)^2 (2\ell_i+1)(\ell_i+1) \times (2\ell_f+1) \begin{pmatrix} \ell_i+1 & \ell_f & \lambda \\ 0 & 0 & 0 \end{pmatrix}^2 \times \begin{Bmatrix} \lambda & \lambda & 1 \\ \ell_i & \ell_i+1 & \ell_f \end{Bmatrix}^2 |M_{\ell_i \ell_f}^{-\lambda-2}|^2. \quad (8)$$

In these excitation functions, the main challenge is the evaluation of the radial matrix elements $M_{\ell_i \ell_f}$, which depend

on the initial ℓ_i and final ℓ_f orbital momenta:

$$M_{\ell_i \ell_f}^{-\lambda-1} = \frac{1}{k_i k_f} \int_0^{\infty} \frac{F_{\ell_i}(k_i r) F_{\ell_f}(k_f r)}{r^{\lambda+1}} dr, \quad (9)$$

where $F_{\ell}(kr)$ is the radial part of the electron wave functions decomposed into partial waves, which are solutions of the wave equation for an unscreened Coulomb potential:

$$\frac{d^2 u_{\ell}(r)}{dr^2} + Q^2(r) u_{\ell}(r) = 0, \quad (10)$$

with

$$Q^2(r) = \frac{2m}{\hbar^2} \left(E + \frac{Ze^2}{r} \right) - \frac{\ell(\ell+1)}{r^2}, \quad (11)$$

where E is the incident electron energy.

In the DWBA method, the scattering states in Eq. (9) are the Coulomb wave functions which at large distances behave as distorted plane waves. This is the case of the DWBA method discussed in Sec. II B. An approximate evaluation of the radial matrix elements can be done by replacing the Coulomb wave functions by simpler ones such as plane waves or WKB wave functions, provided that some validity criteria are fulfilled. The approximation using plane waves is known as the PWBA method. In this paper, we compare three methods, PWBA, WKB, and DWBA, for the evaluation of the radial matrix elements.

A. WKB approximation

The WKB approximation [20,21] is known to give a rather accurate approximation of the radial matrix elements. In hot dense plasmas we are interested in, most of electrons have thermal energies. In that case, standard formulas of the WKB approximation are not sufficient since the entire range for the radial coordinate r has to be considered, including both exponential and oscillatory domains.

Langer [22] derived the following expressions for the radial wave functions on both sides of the turning point r_0 :

$$u_{\ell}(r) = \sqrt{\frac{8\pi\chi(r)}{3Q(r)}} \left\{ \cos\left(\frac{\pi}{3} + \kappa\right) J_{1/3}[\chi(r)] + \cos\left(\frac{\pi}{3} - \kappa\right) J_{-1/3}[\chi(r)] \right\} \quad \text{for } r > r_0, \quad (12)$$

$$u_{\ell}(r) = \sqrt{\frac{8|\chi(r)|}{\pi|Q(r)|}} \left\{ \pi \sin \kappa I_{1/3}[|\chi(r)|] + \cos\left(\frac{\pi}{3} - \kappa\right) K_{1/3}[|\chi(r)|] \right\} \quad \text{for } r < r_0, \quad (13)$$

where κ is an arbitrary constant, and

$$\chi(r) = \int_{r_0}^r Q(r') dr', \quad |\chi(r)| = \int_{r_0}^r |Q(r')| dr'. \quad (14)$$

The functions I , J , and K are the Bessel functions of integer order.

For unscreened Coulomb potential, analytical expressions can be found for $\chi(r)$ and $|\chi(r)|$. However, it is easier to evaluate them fairly accurately with a Gaussian quadrature integration method.

The turning point r_0 is defined as the radius for which Q is equal to zero, that is

$$r_0 = \frac{\hbar^2}{mZe^2} \frac{(\ell + \frac{1}{2})^2}{1 + \sqrt{1 + \frac{2\hbar^2 E(\ell + \frac{1}{2})^2}{mZ^2 e^4}}}. \quad (15)$$

For the approximate resolution of the radial equation, Langer [22] introduces a new variable and a new function which is equivalent to the formal replacement of the term $\ell(\ell + 1)$ by $(\ell + \frac{1}{2})^2$ in both radial equation and turning point expression. One can easily show that on either side of r_0 , the Bessel functions admit asymptotic representations leading to the usual WKB formula.

In the system considered in this paper, each wave function has a unique turning point. As the solution $u_\ell(r)$ must conserve finite values for all r , this imposes that $\kappa = 0$ in Eqs. (12) and (13). Then

$$u_\ell(r) = \frac{1}{2} \sqrt{\frac{8\pi \chi(r)}{3Q(r)}} \{J_{1/3}[\chi(r)] + J_{-1/3}[\chi(r)]\}$$

for $r > r_0$, (16)

$$u_\ell(r) = \frac{1}{2} \sqrt{\frac{8|\chi(r)|}{\pi|Q(r)}} K_{1/3}[|\chi(r)|] \quad \text{for } r < r_0. \quad (17)$$

The radial matrix element contains three contributions:

$$M_{\ell_i \ell_f}^{-\lambda-1} = \frac{1}{k_i k_f} \left[\int_0^{r_i} r^{-\lambda-1} u_{\ell_i}(k_i r) u_{\ell_f}(k_f r) dr + \int_{r_i}^{r_f} r^{-\lambda-1} u_{\ell_i}(k_i r) u_{\ell_f}(k_f r) dr + \int_{r_f}^{\infty} r^{-\lambda-1} u_{\ell_i}(k_i r) u_{\ell_f}(k_f r) dr \right], \quad (18)$$

where r_i and r_f are the turning points of the incoming and outgoing electron waves, respectively. By substituting in Eq. (18) the oscillatory and exponential forms of the function $u_\ell(r)$, one obtains

$$M_{\ell_i \ell_f}^{-\lambda-1} = \frac{\cos^2 \frac{\pi}{3}}{k_i k_f} \left[\int_0^{r_i} r^{-\lambda-1} \frac{8}{\pi} \sqrt{\frac{|\chi_i(r)| |\chi_f(r)|}{|Q_i(r)| |Q_f(r)}} K_{1/3}[|\chi_i(r)|] K_{1/3}[|\chi_f(r)|] dr + \int_{r_i}^{r_f} r^{-\lambda-1} \sqrt{\frac{8\pi \chi_i(r)}{3Q_i(r)}} \sqrt{\frac{8|\chi_f(r)|}{\pi|Q_f(r)}} \{J_{1/3}[\chi_i(r)] + J_{-1/3}[\chi_i(r)]\} K_{1/3}[\chi_f(r)] dr + \int_{r_f}^{\infty} r^{-\lambda-1} \frac{8\pi}{3} \sqrt{\frac{\chi_i(r)}{Q_i(r)}} \frac{\chi_f(r)}{Q_f(r)} \{J_{1/3}[\chi_i(r)] + J_{-1/3}[\chi_i(r)]\} \{J_{1/3}[\chi_f(r)] + J_{-1/3}[\chi_f(r)]\} dr \right]. \quad (19)$$

B. DWBA solution

A simple refinement of the Born approximation is the distorted wave approximation. It uses an exact solution of the radial wave equation, which is the regular Coulomb wave function $F_\ell(kr)$. A more useful expression of the radial matrix element (9) includes an exponential term:

$$M_{\ell_i \ell_f}^{-\lambda-1, q} = \frac{1}{k_i k_f} \int_0^{\infty} \frac{F_{\ell_i}(k_i r) F_{\ell_f}(k_f r)}{r^{\lambda+1}} e^{-qr} dr. \quad (20)$$

The matrix element in Eq. (9) is easily derived from this last one by setting the limit $q \rightarrow 0$.

By expressing the Coulomb wave functions with the integral representation of the confluent hypergeometric function, it is possible to transform the matrix element (20) into the following expression:

$$M_{\ell_i \ell_f}^{-\lambda-1, q} = \frac{|\Gamma(\ell_i + 1 + i\eta_i) \Gamma(\ell_f + 1 + i\eta_f)|}{(2\ell_i + 1)! (2\ell_f + 1)!} \times (\ell_i + \ell_f - \lambda + 1)! i^{\ell_i + \ell_f - \lambda + 2} x^{\ell_i} (-y)^{\ell_f} \times e^{-\frac{\pi(\eta_i + \eta_f)}{2}} (k_i - k_f + iq)^{\lambda-2}$$

$$\times F_2(\ell_i + \ell_f - \lambda + 2, \ell_i + 1 + i\eta_i, \ell_f + 1 - i\eta_f, 2\ell_i + 2, 2\ell_f + 2; x, y), \quad (21)$$

where F_2 denotes the generalized hypergeometric function of the two parameters x and y given by

$$x = \frac{2\eta_f}{\xi + iq \frac{\eta_i}{k_f}}, \quad y = -\frac{2\eta_i}{\xi + iq \frac{\eta_i}{k_f}}. \quad (22)$$

Unfortunately, this F_2 function cannot be easily calculated as its series expansion does not converge. Alder *et al.* [20] already pointed out this difficulty and used hypergeometric functions algebra to derive other expressions.

For those terms whose angular momenta satisfy the condition $\ell_f = \ell_i - \lambda$ (lower band terms), Alder *et al.* [20] obtained:

$$M_{\ell_i \ell_f}^{-\lambda-1} = e^{\frac{\pi}{2}\xi} \left| \frac{\Gamma(\ell + 1 + i\eta_f)}{\Gamma(\ell + \lambda + 1 + i\eta_i)} \right| \left(\frac{\eta_i}{\eta_f} \right)^\ell (2k_i)^{\lambda-2} \times \left\{ 2\text{Re} \left[(-1)^{-\lambda} e^{-\pi\xi} \left(\frac{\xi}{2\eta_f} \right)^{\lambda+i\xi} \right] \times \frac{\Gamma(-\lambda - i\xi) \Gamma(\ell + \lambda + 1 - i\eta_i)}{\Gamma(\ell + 1 - i\eta_f)} \right\}$$

$$\begin{aligned}
 & \times F_2 \left(-\lambda + 1 + i\xi, \ell + \lambda + 1 - i\eta_i, \ell + 1 \right. \\
 & \left. + i\eta_f, \lambda + 1 + i\xi, -\lambda + 1 + i\xi; \frac{\xi}{2\eta_f}, \frac{\xi}{2\eta_f} \right) \Bigg] \\
 & + \frac{|\Gamma(\lambda + i\xi)|^2}{(2\lambda - 1)!} F_2 \left(-2\lambda + 1, \ell + 1 \right. \\
 & \left. + i\eta_f, \ell + 1 - i\eta_f, -\lambda + 1 + i\xi, -\lambda + 1 \right. \\
 & \left. - i\xi; \frac{\xi}{2\eta_f}, \frac{\xi}{2\eta_f} \right) \Bigg\}. \quad (23)
 \end{aligned}$$

For those terms whose angular momenta satisfy $\ell_f = \ell_i + \lambda$ (upper band terms), one gets

$$\begin{aligned}
 M_{\ell\ell+\lambda}^{-\lambda-1} &= e^{-\frac{\pi}{2}\xi} \left| \frac{\Gamma(\ell + 1 + i\eta_i)}{\Gamma(\ell + \lambda + 1 + i\eta_f)} \right| \left(\frac{\eta_i}{\eta_f} \right)^{\lambda-2} (2k_i)^{\lambda-2} \\
 & \times \left\{ 2\text{Re} \left[\left(\frac{2\eta_i}{\xi} \right)^{-\lambda+i\xi} \frac{\Gamma(-\lambda + i\xi)\Gamma(\ell + \lambda + 1 - i\eta_f)}{\Gamma(\ell + 1 - i\eta_i)} \right. \right. \\
 & \times F_2(-\lambda + 1 - i\xi, \ell + \lambda + 1 - i\eta_f, \ell + 1 + i\eta_i, \lambda \\
 & \left. \left. + 1 - i\xi, -\lambda + 1 - i\xi; -\frac{\xi}{2\eta_i}, -\frac{\xi}{2\eta_i}) \right] \right. \\
 & \left. + \frac{|\Gamma(\lambda + i\xi)|^2}{(2\lambda - 1)!} F_2(-2\lambda + 1, \ell + 1 - i\eta_i, \ell + 1 + i\eta_i, -\lambda \right. \\
 & \left. + 1 + i\xi, -\lambda + 1 - i\xi; -\frac{\xi}{2\eta_i}, -\frac{\xi}{2\eta_i}) \right\}. \quad (24)
 \end{aligned}$$

For the general term, with $\ell_i - \lambda < \ell_f < \ell_i + \lambda$, Ohsaki [23] showed that Eq. II.B.62 in [20] is wrong and must be corrected to

$$\begin{aligned}
 M_{\ell_i\ell_f}^{-\lambda-1,q} &= x^{-\ell_i-1} (-y)^{\ell_f} \left| \frac{\Gamma(\ell_f + 1 + i\eta_f)}{\Gamma(\ell_i + 1 + i\eta_i)} \right| \\
 & \times \frac{(2\ell_i)!}{(2\ell_f + 1)! (\ell_i - \ell_f + \lambda - 1)!} \\
 & \times i^{\ell_i - \ell_f + \lambda - 1} (k_i - k_f + iq)^{\lambda-2} \frac{\pi e^{\frac{\pi}{2}\xi}}{\sinh \pi\xi} \\
 & \times F_2(\ell_f - \ell_i + 1 - \lambda, -\ell_i - i\eta_i, \ell_f + 1 \\
 & + i\eta_f, -2\ell_i, 2\ell_f + 2; x, y) \\
 & + x^{\ell_i} (-y)^{-\ell_f-1} \left| \frac{\Gamma(\ell_i + 1 + i\eta_i)}{\Gamma(\ell_f + 1 + i\eta_f)} \right| \\
 & \times \frac{(2\ell_f)!}{(2\ell_i + 1)! (\ell_f - \ell_i + \lambda - 1)!} \\
 & \times i^{\ell_i + \ell_f + \lambda + 1} (k_i - k_f + iq)^{\lambda-2} \frac{\pi e^{-\frac{\pi}{2}\xi}}{\sinh \pi\xi} \\
 & \times F_2(\ell_i - \ell_f + 1 - \lambda, \ell_i + 1 + i\eta_i, -\ell_f - i\eta_f, 2\ell_i \\
 & + 2, -2\ell_f; x, y) - i^{\ell_i + \ell_f + \lambda} x^{\ell_i} (-y)^{\ell_f} \\
 & \times \left| \frac{\Gamma(\ell_f + 1 + i\eta_f)}{\Gamma(\ell_i + 1 + i\eta_i)} \right| \frac{2\pi e^{-\frac{\pi}{2}(\eta_i + \eta_f)}}{\sinh \pi\xi} (k_i - k_f + iq)^{\lambda-2}
 \end{aligned}$$

$$\begin{aligned}
 & \times (1 - x - y)^{-\frac{\ell_i + \ell_f - \lambda + 2}{2}} \text{Re} \left[i(1 - x - y)^{\frac{\ell_i + \ell_f - \lambda + 2}{2}} \right. \\
 & \times \frac{\Gamma(\ell_f + 1 - i\eta_f)}{\Gamma(\ell_i + 1 - i\eta_i)\Gamma(\lambda + 1 - i\xi)} (-x)^{-\ell_i - 1 - i\eta_i} \\
 & \left. \times (-y)^{-\ell_f - 1 - i\eta_f} F_3 \left(\ell_i + 1 + i\eta_i, \ell_f + 1 - i\eta_f, \right. \right. \\
 & \left. \left. - \ell_i + i\eta_i, -\ell_f - i\eta_f, \lambda + 1 - i\xi; \frac{1}{x}, \frac{1}{y} \right) \right]. \quad (25)
 \end{aligned}$$

In these expressions, it is possible to calculate the hypergeometric functions by using their series expansions when the incident electron energy is high enough. However, we also need to be able to calculate them for low-energy electrons, since inelastically scattered electrons under consideration have usually low-energy. Therefore, we used another expression of the general term which uses the Horn function H_2 [23] and whose convergence domain exactly matches the nonconvergence domain of Eq. (25):

$$\begin{aligned}
 M_{\ell_i\ell_f}^{-\lambda-1,q} &= (k_i - k_f + iq)^{\lambda-2} \\
 & \times \frac{|\Gamma(\ell_i + 1 + i\eta_i)\Gamma(\ell_f + 1 + i\eta_f)|\Gamma(-\ell_i + i\eta_i)}{(2\ell_f + 1)!} (-y)^{\ell_f} \\
 & \times \left[e^{-\frac{\pi\xi}{2}} \frac{1}{\Gamma(\lambda - \ell_f + i\eta_i)} i^{\ell_i - \ell_f + \lambda} x^{-1 - i\eta_i} H_2 \right. \\
 & \times \left(\ell_f - \lambda + 1 - i\eta_i, \ell_f + 1 - i\eta_f, \ell_i + 1 \right. \\
 & \left. + i\eta_i, -\ell_i + i\eta_i, 2\ell_f + 2; y, -\frac{1}{x} \right) \\
 & \left. + e^{-\frac{\pi(\eta_i + \eta_f)}{2}} \frac{(2\ell_i)!}{\Gamma(\ell_i + 1 + i\eta_i)(\ell_i - \ell_f + \lambda - 1)!} \right. \\
 & \times i^{\lambda - \ell_i - \ell_f} x^{-\ell_i - 1} F_2(\ell_f - \ell_i - \lambda + 1, \ell_f + 1 - i\eta_f, \\
 & \left. - \ell_i + i\eta_i, 2\ell_f + 2, -2\ell_i; y, x) \right]. \quad (26)
 \end{aligned}$$

The lower band terms do not have convergence problems, but the upper band terms have the same problem as the general terms. In this case, the use of the Horn functions is not possible. As a last resort, we used numerical integration of the matrix element. The integration method involves changing the integration path in the complex plane as proposed by Sil [24]. This method provides satisfactory results but is much more time consuming. So it has been restricted to the only cases where no converging series expansion is available.

Table I sums up all these methods and their validity criteria, based on the convergence of the expansion series of the hypergeometric functions:

TABLE I. Calculation method for the matrix elements.

Term	Condition	Method	Equation
$\ell_f = \ell_i + \lambda$	$E \leq \frac{4}{3}\Delta E$	Sil	see Ref. [24]
	$E > \frac{4}{3}\Delta E$	Alder	(23)
$\ell_i - \lambda < \ell_f < \ell_i + \lambda$	$E < \frac{9}{8}\Delta E$	Ohsaki	(26)
	$E > \frac{9}{8}\Delta E$	Ohsaki	(25)
$\ell_f = \ell_i - \lambda$	All energies	Alder	(24)

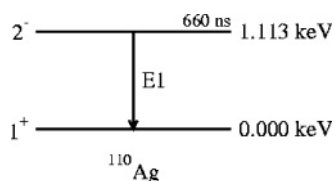


FIG. 1. Simplified level scheme of ^{110}Ag .

III. RESULTS

Typical temperatures of plasma created by today lasers imply that only low-energy nuclear transitions can be excited. A general survey of many nuclear transitions has led to the choice of two nuclei, among others, ^{110}Ag and ^{201}Hg for which we provide detailed results below. The model exposed in Sec. II is used to calculate electron inelastic scattering cross sections.

A. ^{110}Ag

As a first case, we consider the excitation of the ^{110}Ag isomeric state whose level scheme is shown in Fig. 1. It lays 1.113 keV above the ground state, decays down by an E1 transition, and has a lifetime of 660 ns [25].

In Fig. 2, we show the (e, e') excitation cross section as a function of the incident electron energy obtained with DWBA and WKB calculations. We have also added the results of plane wave born approximation (PWBA). The cross section is quite small, never larger than 10^{-29} cm 2 , but in plasma this value is counterbalanced by the high number of free electrons. The three methods exhibit the same behavior for the higher energies whereas they display significant differences near threshold. The DWBA and WKB cross sections do not decrease towards zero when the electron energy is lowering down to the threshold. This well-known behavior of the DWBA approach near threshold [26,27] is explained by the acceleration effect of the electron as it gets close to the nucleus. This artifact will disappear when screening will be taken into account as the global neutrality of the ion and the electronic environment will ensure that this acceleration effect is no

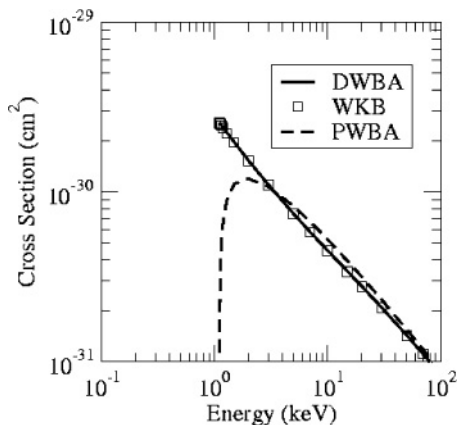


FIG. 2. ^{110}Ag electron inelastic excitation cross section in DWBA (solid line), WKB (squares), and PWBA (dashed line) methods.

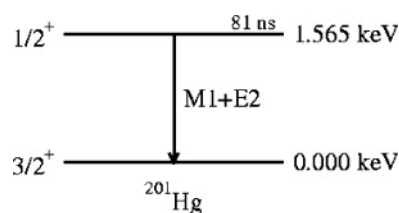


FIG. 3. Simplified level scheme of ^{201}Hg .

longer present. Even though PWBA is a cruder method, it has a better behavior at the threshold for an unscreened nucleus.

DWBA and WKB cross sections are very close to each other, with a difference smaller than 3% within the considered energy range. The treatment by WKB approximation, as proposed by Langer [22], is relevant for this kind of physical situation. Using a solution able to describe the whole radial range including the turning point is much more precise than the usual asymptotic solutions. At this point, let us mention that the maximum orbital momentum required for convergence in the summation of the electron excitation function (7) is around 10 near the threshold, and increases to a few tens for higher energies.

B. ^{201}Hg

We now consider the excitation of the isomeric state of ^{201}Hg whose level scheme is shown in Fig. 3. This state lies 1.565 keV above the ground state, and decays down by a mixed $M1 + E2$ transition [28]. Its lifetime has been recently measured [29] to be 81 ns.

In Fig. 4 is shown the ^{201}Hg excitation cross section as a function of electron energy. Calculations have been performed with the DWBA, WKB, and PWBA methods for the $E2$ transition and only with DWBA and WKB for the $M1$ transition. As for ^{110}Ag , both WKB and DWBA calculations show very similar results. The (e, e') cross section associated with the $M1$ transition is much lower than that for $E2$ transition, as expected from the comparison between the $B(\lambda)$'s for magnetic and electric reduced transition probabilities in ^{201}Hg . For

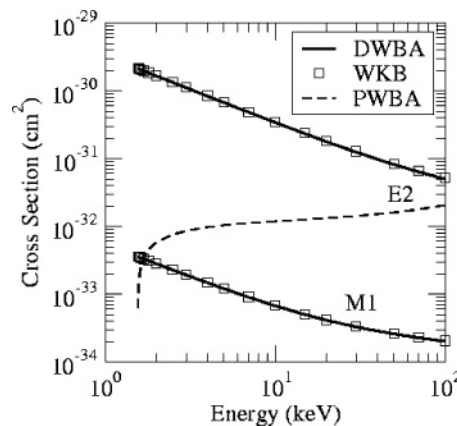


FIG. 4. 1.565 keV level excitation cross section of ^{201}Hg in DWBA (solid line), WKB (squares), and PWBA (dashed line, $E2$ only) methods.

the $E2$ transition, PWBA gives very different result for low energy electrons. At high energy, the PWBA and DWBA cross sections reach the same asymptotic value as expected.

IV. CONCLUSIONS

In this work, we have calculated the cross sections of unscreened inelastic electron scattering in the 1–100 keV range with a DWBA approach using both the exact DWBA solution and a WKB approximation. These two ways of solving the radial wave equation surprisingly give very similar results, with less than 3% difference, here calculated for ^{110}Ag and ^{201}Hg . This conclusion has been found to systematically hold for many nuclei, and is not restricted to the two examples exposed above. We also showed that the simple PWBA approach is not adequate to describe electron inelastic scattering at low energy.

These calculations represent a first step toward the evaluation of electron inelastic scattering in hot dense plasmas. This

will require some description of screening of the electrostatic potential by the bound and the free electrons in the plasma. The cross sections will then have to be calculated using a DWBA approach under the WKB approximation as this method lends itself very well to numerical calculations with a screened potential. A coherent description of the screened cross sections and of the free electron distributions will enable us to calculate the nuclear transition rates in plasma in a fully consistent way.

Experimental evidence of various excitation processes in a plasma remains to be observed. As one step towards this goal, laboratory measurement of the electron inelastic scattering cross section would allow to validate the low energy domain covered by most electrons present in plasma. As only electrons with an energy higher than the nuclear transition energy may contribute to inelastic scattering, only with laser fusion targets near high power lasers, such as future LMJ (Bordeaux, France) or NIF (Livermore, USA), may electron inelastic scattering in plasma be observable.

-
- [1] G. D. Doolen, Phys. Rev. C **18**, 2547 (1978).
 - [2] G. D. Doolen, Phys. Rev. Lett. **40**, 1695 (1978).
 - [3] G. Gosselin, V. Méot, and P. Morel, Phys. Rev. C **76**, 044611 (2007).
 - [4] A. V. Andreev *et al.*, Zh. Eksp. Teor. Fiz. **118**, 1343 (2000) [JETP **91**, 1163 (2000)].
 - [5] A. V. Andreev, A. K. Van'kov, K. Yu. Platonov, Yu. V. Rozdestvenskii, S. P. Chizhov, and V. E. Yashin, Zh. Eksp. Teor. Fiz. **121**, 1004 (2002) [JETP **94**, 862 (2002)].
 - [6] J. J. Niez, C. R. Phys. **3**, 1255 (2002).
 - [7] J. J. Niez and P. Averbuch, Phys. Rev. C **67**, 024611 (2003).
 - [8] M. Schumann, F. Käppeler, R. Böttger, and H. Schölermann, Phys. Rev. C **58**, 1790 (1998).
 - [9] R. A. Ward and W. A. Fowler, Astrophys. J. **238**, 266 (1980).
 - [10] J. J. Carroll, J. A. Anderson, J. W. Glesener, C. D. Eberhard, and C. B. Collins, Astrophys. J. **344**, 454 (1989).
 - [11] A. Coc, M. G. Porquet, and F. Nowacki, Phys. Rev. C **61**, 015801 (1999).
 - [12] M. R. Harston and J. F. Chemin, Phys. Rev. C **59**, 2462 (1999).
 - [13] G. Gosselin and P. Morel, Phys. Rev. C **70**, 064603 (2004).
 - [14] P. Morel, V. Méot, G. Gosselin, D. Gogny, and W. Younes, Phys. Rev. A **69**, 063414 (2004).
 - [15] W. C. Barber, Annu. Rev. Nucl. Sci. **12**, 1 (1962).
 - [16] H. Theissen, *Springer Tracts in Modern Physics* (Springer, Berlin, 1972), Vol. 65, p. 1.
 - [17] E. V. Tkalya, JETP Lett. **53**, 463 (1991).
 - [18] R. V. Arutyunyan, L. A. Bol'shov, A. A. Soldatov, V. F. Strizhov, and E. V. Tkalya, Sov. J. Nucl. Phys. **48**, 827 (1988).
 - [19] V. S. Letokhov and E. A. Yukov, Laser Phys. **4**, 382 (1994).
 - [20] K. Alder, A. Bohr, T. Huus, B. Mottelson, and A. Winther, Rev. Mod. Phys. **28**, 432 (1956).
 - [21] A. Messiah, *Quantum Mechanics* (North Holland, Amsterdam, 1961).
 - [22] R. E. Langer, Phys. Rev. **51**, 669 (1937).
 - [23] A. Ohsaki, T. Kai, E. Kimura, and S. Nakazaki, J. Phys. A **34**, 1935 (2001).
 - [24] N. C. Sil, M. A. Crees, and M. J. Seaton, J. Phys. B **17**, 1 (1984).
 - [25] D. De Frenne and E. Jacobs, Nucl. Data Sheets **89**, 481 (2000).
 - [26] L. A. Vainshtein, I. I. Sobel'man, and E. A. Yukov, *Excitation of Atoms and Spectral Line Broadening* (Nauka, Moscow, 1979).
 - [27] J. A. Tully and D. Petriani, J. Phys. B **7**, 231 (1974).
 - [28] F. G. Kondev, Nucl. Data Sheets **108**, 365 (2007).
 - [29] V. Méot, J. Aupiais, P. Morel, G. Gosselin, F. Gobet, J. N. Scheurer, and M. Tarisien, Phys. Rev. C **75**, 064306 (2007).